Macromolecules

Communication to the Editor

Poly(#-benzyl-l-glutamate) Peptides Confined to Nanoporous Alumina: Pore Diameter Dependence of Self-Assembly and Segmental Dynamics

Hatice Duran, Antonis Gitsas, George Floudas, Mihail Mondeshki, Martin Steinhart, and Wolfgang Knoll

Macromolecules, **2009**, 42 (8), 2881-2885• DOI: 10.1021/ma900119x • Publication Date (Web): 24 March 2009

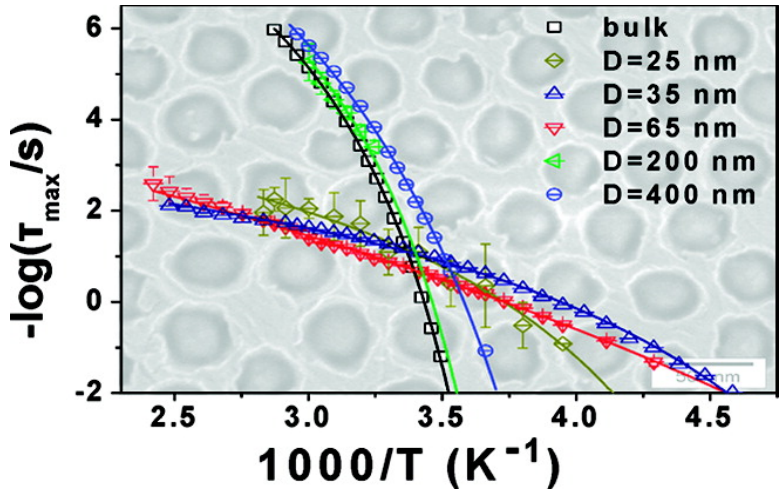

More About This Article

Additional resources and features associated with this article are available within the HTML version:

- Supporting Information
- Access to high resolution figures
- Links to articles and content related to this article
- Copyright permission to reproduce figures and/or text from this article

View the Full Text HTML

Macromolecules

Volume 42, Number 8 April 28, 2009

Communications to the Editor

Poly(γ-benzyl-L-glutamate) Peptides Confined to Nanoporous Alumina: Pore Diameter Dependence of Self-Assembly and Segmental Dynamics

Hatice Duran,[†] Antonis Gitsas,[‡] George Floudas,*[,‡,§] Mihail Mondeshki,[†] Martin Steinhart,[||] and Wolfgang Knoll[†]

Max Planck Institute for Polymer Research, Ackermannweg 10, 55128 Mainz, Germany; Department of Physics, University of Ioannina, 451 10 Ioannina, Greece; Foundation for Research and Technology (FORTH), Biomedical Research Institute, Ioannina, Greece; and Max Planck Institute of Microstructure Physics, Weinberg 2, 06120 Halle, Germany

Received January 19, 2009
Revised Manuscript Received March 8, 2009

Nanoporous hard templates containing arrays of aligned cylindrical channels, such as nanoporous alumina (anodic aluminum oxide, AAO), have been used for the fabrication of nanotubes and nanorods by various techniques, including polymerization of monomers inside the channels[1,2] as well as layer-by-layer deposition of polypeptides and proteins.[3] Nanoporous membranes functionalized with apoenzymes,[4] antibodies,[5,6] and DNA[7] were used for enantioselective separations,[4,5] detection of antigens,[6] and selective DNA permeation with single-base mismatch selectivity.[7] However, macromolecules located inside AAO hard templates may have different segmental dynamics from that in bulk systems that could affect the performance of membrane configurations based on the functionality of biomolecules. Even though dynamics of polymers near interfaces and in thin films has received a great deal of attention,[8] only a few synthetic materials confined to cylindrical nanopores, such as poly(alkylsiloxanes),[9−11] poly(poly(methyl acrylate) (PMA),[12] polystyrene,[13] and liquid crystals,[14−16] have been investigated by different methods, but with different results: enhanced local mobility,[16] unchanged glass temperature but an enhanced chain mobility,[13] whereas in PMA the glass temperature was increased relative to the bulk.[12]

Moreover, previous studies of the dynamics of macromolecules in AAO were predominantly carried out using commercially available filter membranes characterized by disordered arrays of nanopores having diameters D scattered around 200 nm. However, mesophase textures[17] and crystallization of polymers[18−20] in self-ordered AAO hard templates[21] characterized by narrow pore diameter distributions showed a clear dependence on D. Remarkably, little is known as to how pore diameter and rigid pore walls influence the dynamics of biomolecules confined to AAO, even though it is well-known that, for example, the self-organization of polypeptides in the proximity of interfaces is different from that in the bulk.[22,23]

Polypeptides are polymers of exceptional interest because of their close relationship to proteins, their flexibility in functionality, and their molecular recognition properties. They form hierarchically ordered structures containing α-helices, which can be regarded as rigid rods stabilized by intramolecular hydrogen bonds, and β-sheets (stabilized by intermolecular hydrogen bonds) as fundamental secondary motifs.[24,25] Recent dynamic studies of bulk polypeptides as a function of molecular weight and external pressure revealed that the segmental dynamics is associated with the relaxation of amorphous-like segments within the chain and at the chain ends related to broken hydrogen bonds (largely of intramolecular origin).[26,27] A different interpretation emphasizing the side-group mobility has also been provided for the same dynamic process by another group.[28] The existence of (a defected) α-helical secondary structure gives rise to a larger dipole moment parallel to the helical axis that relaxes on a longer time scale.[26−29] Hence, the slower mode reflects the migration of helical sequences along the chain.[27]

In particular, the polypeptide poly(γ-benzyl-L-glutamate) (PBLG) has been studied as a model rigid-rod polymer in solution,[30] in the melt,[26−28,31] and grafted to surfaces.[32] Here we report the strong dependence of the segmental dynamics of PBLG synthesized in self-ordered AAO with mean D values of 25, 35, 65, 200, and 400 nm and a pore depth of 80−95 μm on the pore diameter. Whereas both released PBLG nanorods (by etching the AAO) of all diameters and nanorods located in

* To whom correspondence should be addressed. E-mail: gfloudas@cc.uoi.gr.
[†] Max Planck Institute for Polymer Research.
[‡] University of Ioannina.
[§] Foundation for Research and Technology.
[||] Max Planck Institute of Microstructure Physics.

10.1021/ma900119x CCC: $40.75
Published on Web 03/24/2009

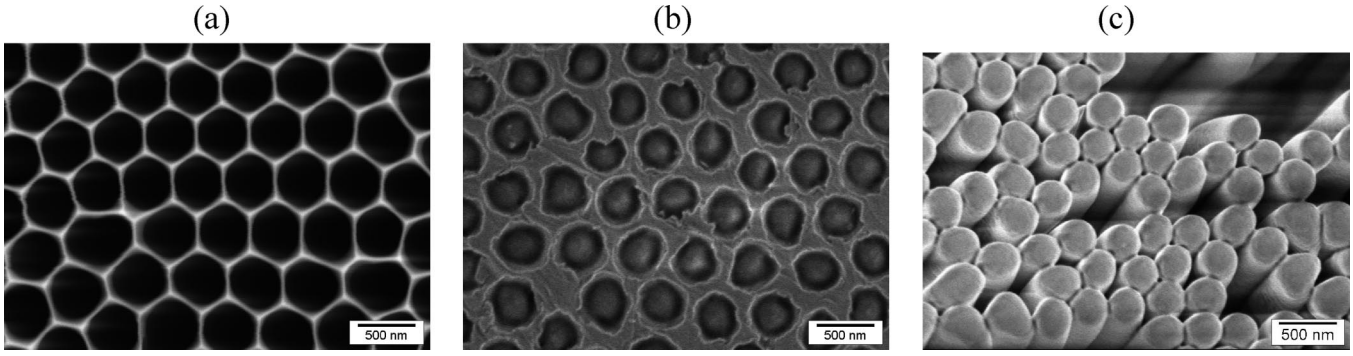

Figure 1. Scanning electron microscopy images of (a) AAO (D = 400 nm) modified with APTES, (b) AAO (D = 400 nm) containing PBLG nanorods, and (c) the same PBLG nanorods released from AAO.

Scheme 1. Synthesis of PBLG Nanorods in Nanoporous AAO

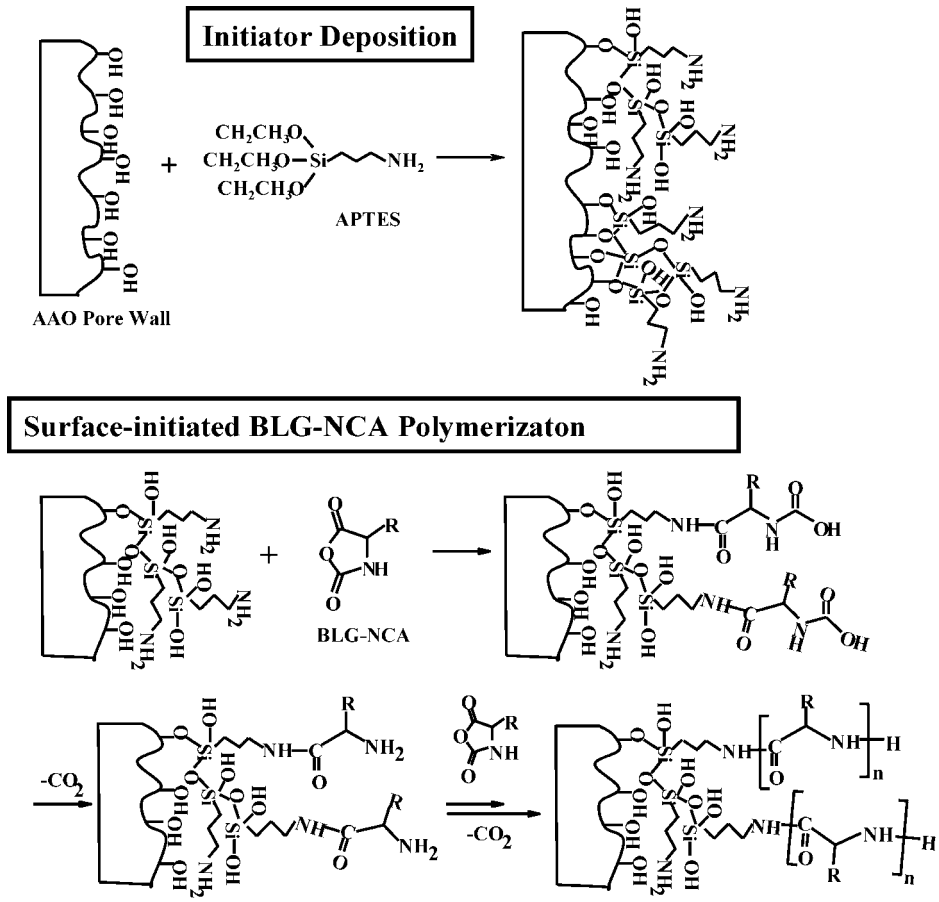

AAO with D values of 200 and 400 nm show bulklike behavior, considerably different segmental dynamics was found for PBLG confined to AAO hard templates with D values equal to or smaller than 65 nm.

PBLG nanorods were synthesized in the pores of AAO hard templates as follows. The AAO was immersed in a 1 vol % solution of dried and distilled 3-aminopropyltriethoxysilane (APTES, obtained from Sigma-Aldrich) in anhydrous ethanol for 6 h, rinsed with anhydrous ethanol, sonicated, and finally baked at 120 °C under argon for 20 min. Under the conditions applied here, it is reasonable to assume that the APTES forms a cross-linked film with a thickness of one to three monolayers (1−3 nm)[33,34] on the pore walls. BLG-NCA monomer was synthesized following procedures reported elsewhere.[35] 100 mM NCA dissolved in 20 mL of anhydrous tetrahydrofuran (THF) was dropped onto the APTES-modified AAO hard templates (Figure 1a) under argon. The polymerization of the infiltrated BLG-NCA into the pores of the AAO (Scheme 1) proceeded overnight at 110 °C under vacuum (1−2 mbar). After the removal of residual material from the top surface of the AAO with sharp blades, the samples were again heated to 100 °C under vacuum for 3 days. Thus, AAO containing PBLG nanorods with uncovered pore openings is obtained (Figure 1b). Optionally, the PBLG nanorods were released by etching the AAO with aqueous 45 wt % hydrofluoric acid solution at 0 °C for 1.5 h and subsequent neutralization of the suspension by several filtration steps (Figure 1c; Figure S1, Supporting Information).

Even in AAO hard templates with the smallest pore diameter of 25 nm, α-helices, which are stable in PBLG containing more than 18 repeat units,[27] were found. Figure 2a displays infrared (IR) spectra of PBLG nanorods residing in AAO with a D value

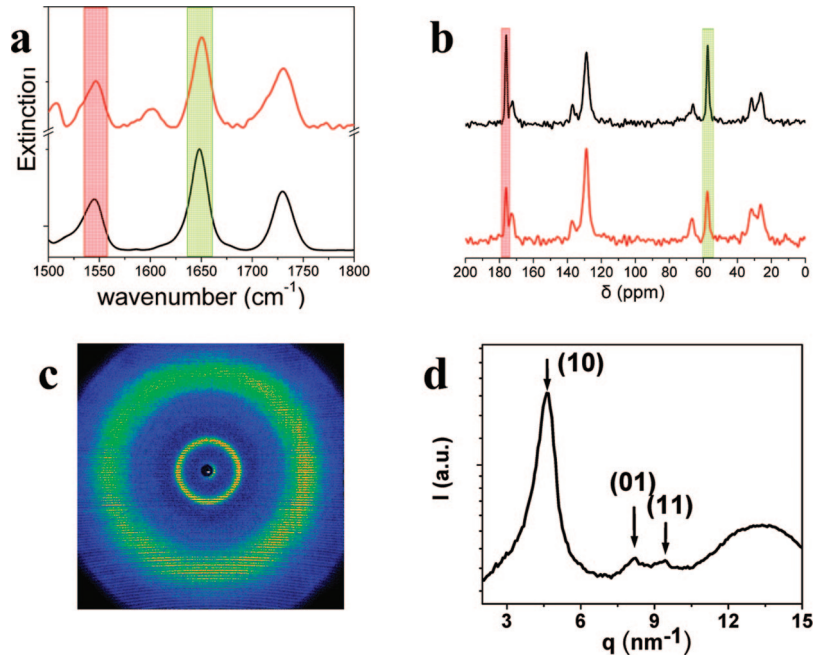

Figure 2. Characterization of the secondary structure of the PBLG nanorods. (a) IR spectra of bulk PBLG with a degree of polymerization of 430 (black line) and of PBLG nanorods located in AAO with a pore diameter of 25 nm (red line). The amide II and amide I bands of PBLG in its α-helical conformation at 1550 and 1650 cm^{-1} are indicated by red and green shading. (b) ^{13}C NMR spectra of PBLG nanorods located in AAO with a pore diameter of 25 nm (bottom) and of PBLG nanorods released from AAO with a pore diameter of 25 nm (top). The intense resonances at $\delta \sim 176$ and 57.5 ppm indicated by red and green shading originate from the carbon atom of the amide carbonyl group and the C_α carbon, respectively, and evidence the presence of PBLG α-helices. (c, d) WAXS patterns of randomly oriented PBLG nanorods released from AAO with a pore diameter of 25 nm after annealing for ~12 h at 433 K and measured at the same temperature. (c) Two-dimensional WAXS pattern; (d) equatorial WAXS intensity profile.

of 25 nm and, for comparison, of bulk PBLG. Both spectra show amide I and II bands at 1650 and 1550 cm^{-1} associated with the α-helical conformation of PBLG. Likewise, ^{13}C chemical shifts (δ) in ^{13}C NMR spectra are very sensitive to the local conformation of peptides.[36] In Figure 2b, characteristic ^{13}C NMR spectra of PBLG nanorods both released from and located in AAO with a D value of 25 nm are seen. The intense resonances at $\delta \approx 176$ and 57.5 ppm arise from the carbon atoms of the amide carbonyl group and from the C_α carbon atoms, respectively, and indicate the presence of α-helical secondary structures. Additional IR and ^{13}C NMR spectra for other pore diameters are given respectively in Figures S2 and S3 (Supporting Information). In all cases the PBLG secondary structure is α-helical. A two-dimensional wide-angle X-ray (WAXS) diffraction pattern of randomly oriented PBLG nanorods released from AAO with a D value of 25 nm after annealing for ~12 h at 433 K and measured at the same temperature is shown in Figure 2c, and a radial intensity profile as a function of the scattering vector q in shown in Figure 2d. The occurrence of a strong peak at $q = 4.6$ nm^{-1} and the higher order peaks can be indexed according to the (10), (01), and (11) reflections of a hexagonal unit cell (the broad feature at around q~14 nm^{-1} originates mainly from the long amorphous side chains of PBLG). Thus, the PBLG helices are arranged in hexagonal structures.[27] Nevertheless, the presence of the peptide secondary structure does not lead to crystallization as the thermal investigation (Figure S4, Supporting Information) revealed only a glass temperature associated with the disordered PBLG segments.

The segmental dynamics of the amorphous-like fraction of the PBLG nanorods was studied by means of dielectric spectroscopy (DS). DS is a versatile technique to probe both segmental dynamics and global chain dynamics of macromolecules interacting with external alternating electric fields.[37] The complex dielectric permittivity $\varepsilon^* = \varepsilon' - i\varepsilon''$, where ε' is the real and ε'' is the imaginary part, is generally a function of frequency ω and temperature T.[37] Both the orientation polarization of permanent dipoles and conductivity contribute to ε^*. The orientational contribution can be fitted using the empirical equation of Havriliak and Negami.[38] Released PBLG nanorods of all diameters and PBLG nanorods located inside AAO hard templates with pore diameters of 400 and 200 nm showed, similar to bulk PBLG,[26] a strong temperature dependence of the segmental dynamics that is well described by the Vogel−Fulcher−Tammann (VFT) equation

$$\tau_{max} = \tau_0 \exp\left(\frac{D_T T_0}{T - T_0}\right) \quad (1)$$

where $\tau_0 = (5.0 \pm 0.5) \times 10^{-12}$ s is the limiting time at very high temperatures, D_T ($= 5.5 \pm 0.2$) is a dimensionless parameter (VFT parameter), and T_0 ($= 241 \pm 1$ K) is the "ideal" glass temperature.

PBLG nanorods located in AAO with pore diameters of 65 nm and below show systematic shifts of the segmental relaxation times relative to bulk PBLG, as it is obvious from the dielectric loss spectra seen in Figure 3a (φ refers to the volume fraction of PBLG within AAO; Supporting Information). At 333 K, the segmental relaxation process of the PBLG nanorods residing in AAO hard templates with a pore diameter of 35 nm appears at ≈50 Hz, a frequency significantly lower than that of the segmental relaxation process of bulk PBLG at $\approx 1 \times 10^5$ Hz. Consequently, the segmental dynamics of PBLG nanorods inside the AAO is slowed down. Below the glass transition temperature of bulk PBLG at 263 K, however, the segmental relaxation process in the PBLG nanorods residing in AAO hard templates with a pore diameter of 35 nm can clearly be detected at ≈3 Hz, whereas the segmental relaxation process of bulk PBLG

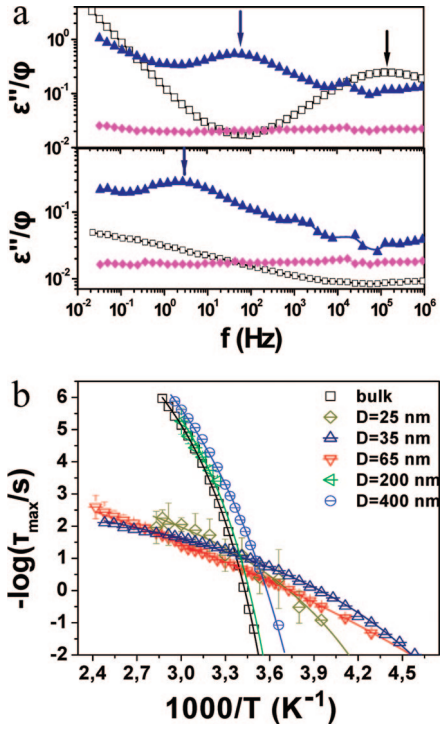

Figure 3. (a) Dielectric loss spectra of bulk PBLG (black open squares) and normalized spectra of PBLG nanorods located in AAO with a D value of 35 nm (blue solid triangles) at 333 K (top) and at 263 K (bottom). The spectra of silanized but empty AAO with a D value of 25 nm (pink solid rhombuses) are also shown for comparison. Notice the shift of the α-process maximum in the nanorods located in the AAO hard templates (indicated by blue arrows) to lower and higher frequencies respectively at 333 and 263 K as compared to bulk PBLG (indicated by the black arrow). (b) Segmental relaxation times plotted in the Arrhenius representation: black squares, bulk PBLG; blue circles with horizontal lines, nanorods located in AAO with a D value of 400 nm; green left triangles with horizontal lines, nanorods located in AAO with a D value of 200 nm; red down triangles with horizontal lines, nanorods located in AAO with a D value of 65 nm; dark blue up triangles with horizontal lines, nanorods located in AAO with a D value of 35 nm; dark yellow rhombuses with horizontal lines, nanorods located in AAO with a D value of 25 nm. The lines are fits to the VFT equation.

lies below 10^{-2} Hz, i.e., outside the experimentally covered frequency range. This indicates that at 263 K the segmental relaxation in PBLG nanorods inside AAO is faster than in bulk PBLG (a process due to surface polarization appears at much lower frequencies). Dielectric loss spectra of silanized but empty AAO with a pore diameter of 35 nm, which are shown in Figure 3a for comparison, are essentially featureless so that artifacts such as presence of water or other contaminants can be ruled out.

Figure 3b displays an Arrhenius plot of the segmental relaxation times $\tau(T)$ of disordered PBLG segments in PBLG nanorods confined to AAO with various pore diameters as a function of the inverse temperature. Bulk PBLG and the PBLG located in AAO with D values of 200 and 400 nm show typical "fragile" dynamic behavior, that is, pronounced $\tau(T)$ dependence. The VFT parameters of PBLG residing in pores with D values of 400 and 200 nm deviate only slightly from that of bulk PBLG. Strikingly, PBLG confined to pores with D values between 25 and 65 nm exhibits completely different segmental dynamics characterized by "strong" dynamic behavior with a significantly weaker dependence of the segmental relaxation times on the temperature. Moreover, the glass temperatures, T_g (defined as the temperature where the segmental relaxation time is at $\tau \sim 10$ s), are reduced by as much as 50 K relative to that of bulk PBLG or PBLG located in AAO with pore diameters of 200 and 400 nm.

The steepness index m,[39] defined as $m = \mathrm{d}(\log \tau)/\mathrm{d}(T_g/T)$ and determined at T_g, decreases from a bulk value of ≈65 to a value of ≈10. Such significant changes in the temperature dependence of the segmental dynamics have been reported for some synthetic polymers[40,41] whereas no change has been reported by other groups.[42,43] We mention here that this effect cannot be caused by the fixation of one chain end at the pore walls since no such effect has been observed in copolypeptides.[29] Independent density measurements of the PBLG inside AAO pores using a microbalance (Supporting Information) revealed insensitivity to pore diameter. In addition, increased density of the PBLG inside the pores can be ruled out as densification leads to an increase of T_g.[26] Remarkably, the glass transition in released PBLG nanorods of any diameter occurs at the bulk glass temperature of PBLG of about 284 K (Figure S5, Supporting Information), and they show "fragile" $\tau(T)$ dependence like bulk PBLG. Apparently, it is the presence of the rigid pore walls in AAO with pore diameters of 65 nm and below that induces the change of segmental dynamics rather than the geometric confinement itself. In a strong and irreversible adsorption scenario, i.e., when the sticking energy of a repeat unit exceeds the thermal energy, k_BT, chains can be trapped in unusual long-lasting conformations. It is reasonable to assume that the pore walls of the AAO hard templates are screened by the APTES layer, but unreacted ethoxy groups of the APTES are prone to hydrolysis,[33,34] and the silanol groups thus formed (Scheme 1) can form hydrogen bonds with the amide groups of the polypeptide chains. The propensity for hydrogen bonding between carbonyl groups and hydroxyl groups is well-known. Thus, the weak $\tau(T)$ dependence in the present case has a different origin than the one discussed earlier; it results from the redistribution of hydrogen bonds of the polypeptide backbone with the silanol groups. The additional hydrogen bonds disrupt the backbone conformations and are also responsible for the absence of the slower process associated with the migration of helical sequences along the chain.

In conclusion, nanorods consisting of the polypeptide PBLG were synthesized in nanoporous AAO hard templates with pore diameters ranging from 25 to 400 nm. Independent of the pore diameter of the AAO, the PBLG nanorods contained α-helical PBLG segments packed in hexagonal superstructures in the absence of long-range order. The segmental dynamics of PBLG located in AAO with pore diameters of 200 and 400 nm, as well as of PBLG nanorods of all diameters released from the AAO hard templates, corresponded to that of bulk PBLG characterized by "fragile" temperature dependence of the relaxation times. A striking change from "fragile" to "strong" dynamic behavior occurred if PBLG was confined to AAO hard templates with pore diameters equal to or smaller than 65 nm. A distinct change of the dynamic behavior rather than a gradually increasing interphase contribution was observed. The temperature dependence of segmental dynamics became significantly weaker than in case of bulk PBLG, and the effective glass temperature was reduced by as much as 50 K. Both are discussed in terms of the newly formed hydrogen bonds between the silanol groups and the peptide backbone. Therefore, these results have to be considered when designing membrane configurations based on the functionality of biopolymers located in nanopores. Lastly, the altered segmental mobility of PBLG within the smaller pores was confirmed by independent variable temperature ^{1}H NMR measurements that will be reported elsewhere in detail.[44]

Acknowledgment. Technical support by R. Brandscheid, B. Yameen, G. Glasser, S. Sklarek, and S. Kallaus and funding by the Greek General Secretariat for Research and Technology (PENED2003/856) and the German Research Foundation (Priority Program 1369 "Polymer-Solid Contacts: Interfaces and Interphases") are gratefully acknowledged. H.D. thanks the European Union for a Marie Curie Intra-European Fellowship (MEIF-CT-2005-024731).

Supporting Information Available: Experimental details of the characterization of the PBLG nanorods (scanning electron microscopy, Fourier transform infrared spectroscopy, solid-state NMR, wide-angle X-ray scattering, thermal behavior, density measurements, dielectric spectroscopy). This material is available free of charge via the Internet at http://pubs.acs.org.

References and Notes

(1) Cai, Z.; Martin, C. R. *J. Am. Chem. Soc.* **1989**, *111*, 4138.
(2) Liang, W.; Martin, C. R. *J. Am. Chem. Soc.* **1990**, *112*, 9666.
(3) Hou, S. F.; Wang, J. H.; Martin, C. R. *Nano Lett.* **2005**, *5*, 231.
(4) Lakshmi, B. B.; Martin, C. R. *Nature (London)* **1997**, *388*, 758.
(5) Lee, S. B.; Mitchell, D. T.; Trofin, L.; Nevanen, T. K.; Soderlund, H.; Martin, C. R. *Science* **2002**, *296*, 2198.
(6) Dai, J. H.; Baker, G. L.; Bruening, M. L. *Anal. Chem.* **2006**, *78*, 135.
(7) Kohli, P.; Harrell, C. C.; Cao, Z. H.; Gasparac, R.; Tan, W. H.; Martin, C. R. *Science* **2004**, *305*, 984.
(8) Forrest, J. E.; Jones, R. A. L. In *Polymer Surfaces, Interfaces and Thin Films*; Karim, A., Kumar, S., Eds.; Word Scientific: Singapore, 2000. Special Issue on "Dynamics in Confinement": Frick, B., Koza, M., Zorn, R. Eds. [*Eur. Phys. J. E* **2003**, *12*, 5]; Special Issue on "Properties of Thin Polymer Films": Reiter, G., Forrest, J. A., Eds. [*Eur. Phys. J. E* **2002**, *8*, 101].
(9) Cosgrove, T.; Prestidge, C. A.; Vincent, B. *J. Chem. Soc., Faraday Trans.* **1990**, *86*, 1377.
(10) Primak, S. V.; Jin, T.; Dagger, A. C.; Finotello, D.; Mann, E. K. *Phys. Rev. E* **2002**, *65*, 031804.
(11) Jagadeesh, B.; Demco, D. E.; Blümich, B. *Chem. Phys. Lett.* **2004**, *393*, 416.
(12) Okuom, M. O.; Metin, B.; Blum, F. D. *Langmuir* **2008**, *24*, 2539.
(13) Shin, K.; Obukhov, S.; Chen, J.-T.; Huh, J.; Hwang, Y.; Mok, S.; Dobriyal, P.; Thiyagarajan, P.; Russell, T. P. *Nature (London)* **2007**, *6*, 961.
(14) Crawford, G. P.; Ondris-Crawford, R. J.; Doane, J. W.; Žumer, S. *Phys. Rev. E* **1996**, *53*, 3647.
(15) Rozanski, S. A.; Stannarius, R.; Groothues, H.; Kremer, F. *Liq. Cryst.* **1996**, *20*, 59.
(16) Brás, A. R.; Dionísio, M.; Schönhals, A. *J. Phys. Chem. B* **2008**, *112*, 8227.
(17) Steinhart, M.; Zimmermann, S.; Göring, P.; Schaper, A. K.; Gösele, U.; Weder, C.; Wendorff, J. H. *Nano Lett.* **2005**, *5*, 429.
(18) Steinhart, M.; Göring, P.; Dernaika, H.; Prabhukaran, M.; Gösele, U.; Hempel, E.; Thurn-Albrecht, T. *Phys. Rev. Lett.* **2006**, *97*, 027801.
(19) Woo, E.; Huh, J.; Jeong, Y. G.; Shin, K. *Phys. Rev. Lett.* **2007**, *98*, 136103. Shin, K.; Woo, E.; Jeong, Y. G.; Kim, C.; Huh, J.; Kim, K.-W. *Macromolecules* **2007**, *40*, 6617.
(20) Ma, Y.; Hu, W.; Hobbs, J.; Reiter, G. *Soft Matter* **2008**, *4*, 540.
(21) Masuda, H.; Fukuda, K. *Science* **1995**, *268*, 1466. Masuda, H.; Hasegawa, F.; Ono, S. *J. Electrochem. Soc.* **1997**, *144*, L127. (bb) Masuda, H.; Yada, K.; Osaka, A. *Jpn. J. Appl. Phys., Part 2* **1998**, *37*, L1340.
(22) Rapaport, H.; Kjaer, K.; Jensen, T. R.; Leiserowitz, L.; Tirrell, D. A. *J. Am. Chem. Soc.* **2000**, *122*, 12523.
(23) Jaworek, T.; Neher, D.; Wegner, G.; Wieringa, R. H.; Schouten, A. J. *Science* **1998**, *279*, 57.
(24) Walton, A. G.; Blackwell, J. In *Biopolymers*; Academic Press: New York, 1973.
(25) Block, H. In *Poly(γ-benzyl-L-glutamate) and Other Glutamic Acid Containing Polymers*; Gordon and Breach Science Publishers: New York, 1983.
(26) Papadopoulos, P.; Floudas, G.; Schnell, I.; Klok, H.-A.; Aliferis, T.; Iatrou, H.; Hadjichristidis, N. *J. Chem. Phys.* **2005**, *122*, 224906. Floudas, G.; Spiess, H. W. *Macromol. Rapid Commun.* **2009**, *30*, 278.
(27) Papadopoulos, P.; Floudas, G.; Klok, H.-A.; Schnell, I.; Pakula, T. *Biomacromolecules* **2004**, *5*, 81.
(28) Hartmann, L.; Kratzmuller, T.; Braun, H.-G.; Kremer, F. *Macromol. Rapid Commun.* **2000**, *21*, 814.
(29) Floudas, G.; Papadopoulos, P.; Klok, H.-A.; Vandermeulen, G. W. M.; Rodriguez-Hernandez, J. *Macromolecules* **2003**, *36*, 3673. Gitsas, A.; Floudas, G.; Dietz, M.; Mondeshki, M.; Spiess, H. W.; Wegner, G. *Macromolecules* **2007**, *40*, 8311.
(30) Wada, A. *J. Chem. Phys.* **1958**, *29*, 674; **1959**, *30*, 328; **1959**, *30*, 324.
(31) Schmidt, A.; Lehmann, S.; Georgelin, M.; Katana, G.; Mathauer, K.; Kremer, F.; Schmidt-Rohr, K.; Boeffel, C.; Wegner, G.; Knoll, W. *Macromolecules* **1995**, *28*, 5487.
(32) Wieringa, R. H.; Siesling, E. A.; Werkman, P. J.; Angerman, H. J.; Vorenkamp, E. J.; Schouten, A. J. *Langmuir* **2001**, *17*, 6485.
(33) Kurth, D. G.; Bein, T. *Langmuir* **1995**, *11*, 3061.
(34) Jonas, U.; Krüger, C. *J. Supramol. Chem.* **2002**, *2*, 255.
(35) Daly, W. H.; Poché, D. *Tetrahedron Lett.* **1988**, *29*, 5859.
(36) Shoji, A.; Ozaki, T.; Saito, H.; Tabeta, R.; Ando, I. *Macromolecules* **1984**, *17*, 1472.
(37) Kremer, F., Schönhals, A., Eds.; *Broadband Dielectric Spectroscopy*; Springer: Berlin; 2002. Riande, E.; Diaz-Calleja *Electrical Properties of Polymers*; Marcel Dekker: New York, 2004.
(38) Havriliak, S.; Negami, S. *Polymer* **1967**, *8*, 161.
(39) Böhmer, R.; Ngai, K. L.; Angell, C. A.; Plazek, D. J. *J. Chem. Phys.* **1993**, *99*, 4201.
(40) Schönhals, A.; Goering, H.; Schick, C.; Frick, B.; Zorn, R. *Colloid Polym. Sci.* **2004**, *282*, 882; *J. Non-Cryst. Solids* **2005**, *351*, 2668.
(41) Fakhraai, Z.; Forrest, J. A. *Phys. Rev. Lett.* **2005**, *95*, 025701.
(42) Serghei, A.; Huth, H.; Schick, C.; Kremer, F. *Macromolecules* **2008**, *41*, 3636.
(43) Zhou, D.; Huth, H.; Gao, Y.; Xue, G.; Schick, C. *Macromolecules* **2008**, *41*, 7662.
(44) Gitsas, A.; Duran, H.; Floudas, G.; Mondeshki, M.; Spiess, H. W.; Steinhart, M.; Knoll, W., in preparation.

MA900119X